Supporting Information

4D-Printed Multifunctional Hydrogels as Flexible Strain Sensors and Nerve Conduits

Akshat Joshi[1*], Saswat Choudhury[1*], Arabinda Majhi[2], Sampath Parasuram[3], Vageesh Singh Baghel[4], Samrat Chauhan[5], Supriya Khanra[5], Debrupa Lahiri[2], Kaushik Chatterjee[1,3#]

[1]Department of Bioengineering, Indian Institute of Science, C.V. Raman Avenue, Bangalore, India 560012

[2]Biomaterials and Multiscale Mechanics Lab, Department of Metallurgical and Materials Engineering, Indian Institute of Technology Roorkee, Roorkee, 247667 India

[3]Department of Materials Engineering, Indian Institute of Science, C.V. Raman Avenue, Bangalore, India 560012

[4]Department of Mechanical Engineering, Indian Institute of Science, Bangalore, 560012 India

[5]Chitkara College of Pharmacy, Chitkara University, Punjab 140401 India

*equal contribution

#Corresponding author:

kchatterje@iisc.ac.in; +91-80-22933408

1. Materials and Methods

1.1 Functionalization of CNTs into carboxylic acid-modified CNTs (fCNTs)

As-received CNTs (NC7000, purchased from Nanocyl SA, Belgium) were subjected to acidic oxidation using a mixture of concentrated sulfuric and nitric acid (in the volume ratio of 1:3). Briefly, 200 mL of acid solution was made into which 1 g CNT was introduced and kept under constant stirring for 6h at 80°C, after which it was cooled to room temperature, diluted using DI water, and filtered using Whatman filter paper. The obtained residue was repeatedly washed with DI water to remove any residual acid till a neutral pH was obtained. The acid-functionalized CNT particles (fCNTs) were dried in a vacuum oven at 60 °C for 24h.

1.2 Fabrication of the composite fCNT-hydrogel-based NGC

The neat hydrogels comprising alginate and methyl cellulose of two different compositions (3:9 and 4: 6) were prepared as previously reported. For the composite gels, fCNT was dispersed in DI water via probe sonication for 20 min. Alginate and methyl cellulose powders were dissolved in the fCNT dispersion under constant stirring at 70°C. The resulting homogeneous solution was then filled in a cartridge used for 3D printing and was kept at 4ºC for 30 min for complete hydration of MC, following which the cartridge was stored at room temperature (25ºC) until further use. For preparing the composite alginate/methylcellulose:4/6 gels, a similar procedure was followed with 5 mM $BaCl_2$ solution replacing DI water.

1.3 3D Printing and characterization of the fCNT-gel

3D printing of fCNT-gel

3D models were designed in Solidworks (Dassault System), which were converted to StereoLithography (.Stl) format for slicing to generate G-codes (Repetier Host, CELLINK). For creating the G-codes, the print paths were defined as per computational designs, wherein a

first solid layer of fCNT: 3/9 was overlaid by stripes of fCNT: 4/6 placed at an angle of 90° on

the second and third layers with respect to the first layer. For creating stripes, 40% aligned rectilinear infill patterns with defined fill angles were used, as per computational design. The resulting G-codes were then input to an extrusion-based 3D bioprinter (BioX, CELLINK) for 3D printing of the gels independently from two nozzles of 250 µm. The printed constructs were air-dried for 8 h at RT and immersed in 200 mM

$BaCl_2$ solution. The resulting shape changes were recorded digitally.

Physicochemical characterization of fCNT-gel

The pore morphology of both the composite gels was characterized using a scanning electron microscope (JEOL SEM IT 300) after lyophilization and then sputter-coating with gold. For the cross-sectional SEM of the dual component gels, a transverse slice was cut from the lyophilized gel sample and observed. Swelling studies were performed after drying the gels overnight. The initial dry weight (W_0) of the gels was measured and then soaked in 200 mM $BaCl_2$ solution. The weight (W_t) of the gels was monitored at regular intervals till the weight remained constant. The extent of swelling was calculated using the equation:

$$Swelling\ (\%) = \frac{W_t - W_0}{W_t} \times 100$$

Rheological measurements were performed using a rotational rheometer (Anton Paar Modular Compact Rheometer- 302) with a 10 mm parallel plate and 1 mm gap. For the viscosity flow test, the viscosity of the gels was measured at shear rates ranging from 1 to 100 s^{-1}. For the angular frequency sweep, a constant strain of 1% was chosen from the linear viscoelastic region (LVR), and angular frequency was varied from 1 to 100 rad s^{-1}. Thixotropy characterization was performed in three steps: a low shear rate of 0.1 s^{-1} was applied to the gels for 60 s, the shear rate was increased to 100 s^{-1} for 10s, and finally, the shear rate was lowered to 0.1 s^{-1} for 60 s.

Micro-computed tomography (μ-CT) of fCNT-gel

The self-rolled hollow tubes, crosslinked with $BaCl_2$ solution, were imaged by high-resolution X-ray Micro-Computed Tomography (μCT, Xradia) with a Hamamatsu X-ray source. The source voltage was set at 50 kV, power at 4 kW, and the beam exposure time was 1.5s. The hollow NGC was scanned to obtain a series of 2D cross-section images with a spatial resolution. These 2D images were then reconstructed and analyzed using TXM3D Viewer 1.2.7 software.

Electrical conductivity of fCNT gel

The 3D-printed hydrogel discs (10 mm diameter and 2 mm height) of neat and fCNT (1 and 2 mg/mL) were used to measure the AC conductivity using an Alpha-Aanalyzer (Novocontrol, Germany) in a broad range of frequencies varying from 10^{-1} to 10^{6} Hz. A bulk electrical conductivity measurement was performed across the thickness of the hydrogel samples. At least three samples were tested for each group. For strain sensing experiments, a source meter (Keithley Model 2400) was used to capture the change in resistance in the printed fCNT-gels while they are subjected to different kinds of mechanical deformations.

1.4 Finite Element Analysis (FEA) theory and simulations

The structure which is needed to create the necessary conduit can bend out of the plane due to a differential swelling ratio in the two-layer system. The encoding orientations of the uniformly spaced "strands" in the top layer determine the desired deformation patterns of behavior. An equivalent thermal expansion model has been employed to simulate the swelling processes of a two-layer hydrogel design in order to predict its final shape. Fick's law governs swelling, while Fourier's law governs heat transfer. Since both governing principles are diffusive, a thermal expansion model may be used to simulate hydrogel swelling. This equivalence establishes a connection between the hydrogel structure's material as well as geometrical

characteristics with the thermally expanding structure. We simulate a bottom layer with 100% infill density of higher swelling ratio hydrogel (fCNT:3/9) and a top layer with 40% infill density of lower swelling ratio hydrogel (fCNT:4/6). We design the structure of the same dimensions for simulations as we do for the experiments. Additionally, we observe that the two-layer hydrogel system undergoes large deformation when it swells; therefore, the simulations take geometric nonlinearity into account. By applying Timoshenko's analytical formula for the out-of-plane deformation of bimetallic strips, we were able to correlate the material properties of the hydrogel with those of the thermally expanding one.

Once the equivalence between the structures used in the experiment and simulation is achieved, we prepare 3D models in SolidWorks (Dassault Systems) to capture the encoding directions. We imported the designs into the commercially available finite element analysis (FEA) software program Abaqus 2017 (Simulia) to predict the deformation of the hydrogel structure. We employ quadratic tetrahedron elements from a 3D stress family with 10 nodes (C3D10) for FEA in standard and explicit models. We use a static general solver with a full Newton solution technique to produce the steady state deformation of a two-layer hydrogel structure.

Different 3D models were prepared in Solidworks (Dassault Systems), which were then imported into the commercially available FEA software package (Abaqus 2017, Simulia 2017) to predict the deformation of the hydrogel designs experimentally.

1.5 *In vitro* cell culture and cytocompatibility and staining assays on fCNT-gels

HT-22 cells (mouse hippocampal neuronal cells) were cultured and maintained in Minimum Essential Medium (MEM) obtained from HiMedia, India. The medium was completed with 10 % fetal bovine serum (FBS) sourced from Gibco, Thermo Fisher Scientific, USA, in addition to 1 % antibiotic solution containing penicillin (100 U/ml) and streptomycin (100 mg/ml) obtained from HiMedia, Mumbai, India. The process of cell trypsinization was

performed when the cells reached a confluency level of 60–70 %. This was achieved by utilizing a solution containing 0.25 % trypsin. The cells were cultured under controlled conditions at a temperature of 37 °C with a CO_2 concentration of 5% and 95% relative humidity. The 3D-printed gels were sterilized under UV for 1 h prior to cell seeding. TCP denotes the tissue culture plate, which functions as a control group for baseline comparisons with the experimental groups: gel and fCNT-gel.

Calculation of % cell survival/viability is done by first subtracting the absorbance values of media only from the absorbance values of Alamar Blue in media. This gives the absorbance of Alamar Blue in media – absorbance of media only.

AO_{LW} = absorbance of oxidized form at lower wavelength (570 nm)

and AO_{HW} = absorbance of oxidized form at higher wavelength (600 nm)

Correction factor: $R_0 = AO_{LW}/ AO_{HW}$.

To calculate the % of reduced Alamar Blue:

$AR_{LW} = A_{LW} – (A_{HW} \text{ x } R_0) \text{ x } 100$

The % difference between the experimental sample and control (i.e. TCP) in cytotoxicity/proliferation assays then gives the % cell survival:

$$\% \text{ cell survival} = \frac{A_{LW} - (A_{HW} \times R_0)\ for\ sample}{A_{LW} - (A_{HW} \times R_0)\ for\ control} \times 100$$

1.6 *In Vivo* Studies on the Sciatic Nerve Transected Model

Adult Sprague-Dawley male rats (between 250-270 grams at the time of surgery) were selected to estimate the efficacy of fabricated scaffolds in the regeneration of PNS involving the earlier described sciatic nerve injury model, as described earlier. A total of 16 animals were arbitrarily

divided into four groups: sham-operated (operational control), negative control (injury without any treatment given), gels (4D-printed neat gels), and fCNT-gels (4D-printed conducting fCNT-gels). The resulting dimensions of the self-folding sheets were predicted using simulations to yield conduits to sufficiently cover the defect. Each group contained four animals. Sciatic nerve regeneration was investigated in this work using an injury model with a 5 mm transection. Both NGCs, gel and fCNT-gel, were sterilized through UV irradiation. Before transplantation, the flat sheets of gel and fCNT-gel were exposed to 200 mM of $BaCl_2$ solution and placed at the defect site. Thereafter, 5 mM $BaCl_2$ was poured over the sheets to induce self-folding into tubular structures spontaneously around the injured nerve due to the pre-programmed deformation. Intraperitoneal injections of ketamine (90 mg/kg) and xylazine (10 mg/kg) were used to anesthetize the animals, followed by a bilateral incision at the left lateral thigh. The sciatic nerve was uncovered by cutting through the biceps femoris and gluteus superficialis muscles. Each rat had a 5 mm nerve deficit, which was then bridged utilizing different neural scaffolds. Nerve conduits were used to connect the proximal and distal ends of the damaged nerve. As the conduits were wrapped automatically around the wound, no suturing was required. A 5-mm segment of the sciatic nerve was removed, and the two ends were left untreated for the negative group. The muscle and skin layers were appropriately sutured with 30 nylon sutures after the implant site had been cleaned and disinfected. To avoid infection, each rat was administered 800,000 units of penicillin immediately following surgery.

Sciatic Functional Index (SFI)

SFI was determined from this formula:

$$SFI = 38.3 \times (EPL-NPL)/NPL + 109.5 \times (ETS-NTS)/NTS$$

$$+13.3 \times (EIT-NIT)/NIT-8.8$$

where PL indicates the footprint length, TS denotes the total toe spread, IT stands for intermediate toe spread, E is the injured side, and N represents the distance on the contralateral side.

Tissue Collection

The animals were sacrificed after eight weeks post-implantation via dislocation of the cervical vertebrae to harvest the tissues. The surgical site was opened up to isolate the NGC-wrapped area of the resected sciatic nerve in each rat. After separation, the nerve conduits containing the regenerated neural tissues were fixed with 10% neutral-buffered formalin (NBF) at RT for 24 h. The fixed tissues were used for immunohistochemistry (IHC) and hematoxylin−eosin (H&E) staining. Gastrocnemius muscles of the operated left legs were collected for wet weight measurement and HE staining.

H&E and IHC Staining

Eight weeks post-implantation, the regenerated nerves in the conduits were examined histologically. 5 μm-thick longitudinal and cross sections were cut from the fixed samples using a microtome (Leica) and embedded in paraffin wax. The sections were deparaffinized with xylene and with a gradient of diluted ethanol (100, 90, 70, and 50%). They were further rehydrated, which was followed by gentle rinsing in tap water and staining with freshly prepared HE62. The sections were dried and mounted on coverslips in DPX (di-styrene, a plasticizer, and xylene) (SRL, India). A microscope with RGB (Red, Green, Blue) filters (Lionheart LX, BioTek, USA) was used to image the stained sections to observe the morphology of regenerated nerve tissues.

Immunofluorescence was performed on cross-sections as well as longitudinal sections taken from the central portion of the regenerated tissues in the conduit after staining for NF200 and S-100. The procedure described above for immunohistochemistry staining was used. After

rehydration, antigen retrieval was carried out by incubating for 3 minutes under moist pressure in sodium citrate buffer (pH 6). After rinsing in Tris-buffered saline (pH 7.6), the sections were dried. 1% BSA was used for 2 h as a blocking agent, followed by overnight incubation with mouse monoclonal NF-160 (Sigma-Aldrich, USA) and rabbit polyclonal S100 (Invitrogen, USA) at 4°C. The sections were washed with Tris-buffered saline containing 0.1% Tween® 20 Detergent (TBST) and incubated with rabbit anti-mouse IgG (H + L) − fluorescein isothiocyanate conjugate (Thermo, USA) secondary antibody for NF-160 and the goat antirabbit IgG (H + L) −tetramethylrhodamine isothiocyanate conjugate (Thermo, USA) secondary antibody for S100 for 2 h followed by washing with TBST. The sections were counterstained with DAPI (HiMedia). Finally, the samples were observed using an epi-fluorescence microscope (Lionheart LX, BioTek, USA). At least three areas were sampled for each section/group.

Statistical analysis:

All experiments were performed in triplicate, and the results are shown as the mean ± standard error for each. GraphPad Prism 5.04 was used for the statistical analysis (GraphPad Software, San Diego, CA, USA). One-way ANOVA was used for the statistical analysis, which was then followed by Dunnett and Tukey tests for significance. All analyses were carried out at a 95% confidence level and were considered to be significant at a statistical probability (p-value) <0.05. Statistical significances were denoted as (*/#/@), (**/##/@@) and (***/###/@@@) for $p < 0.05$, $p < 0.01$ and $p < 0.001$, respectively.

2. Results

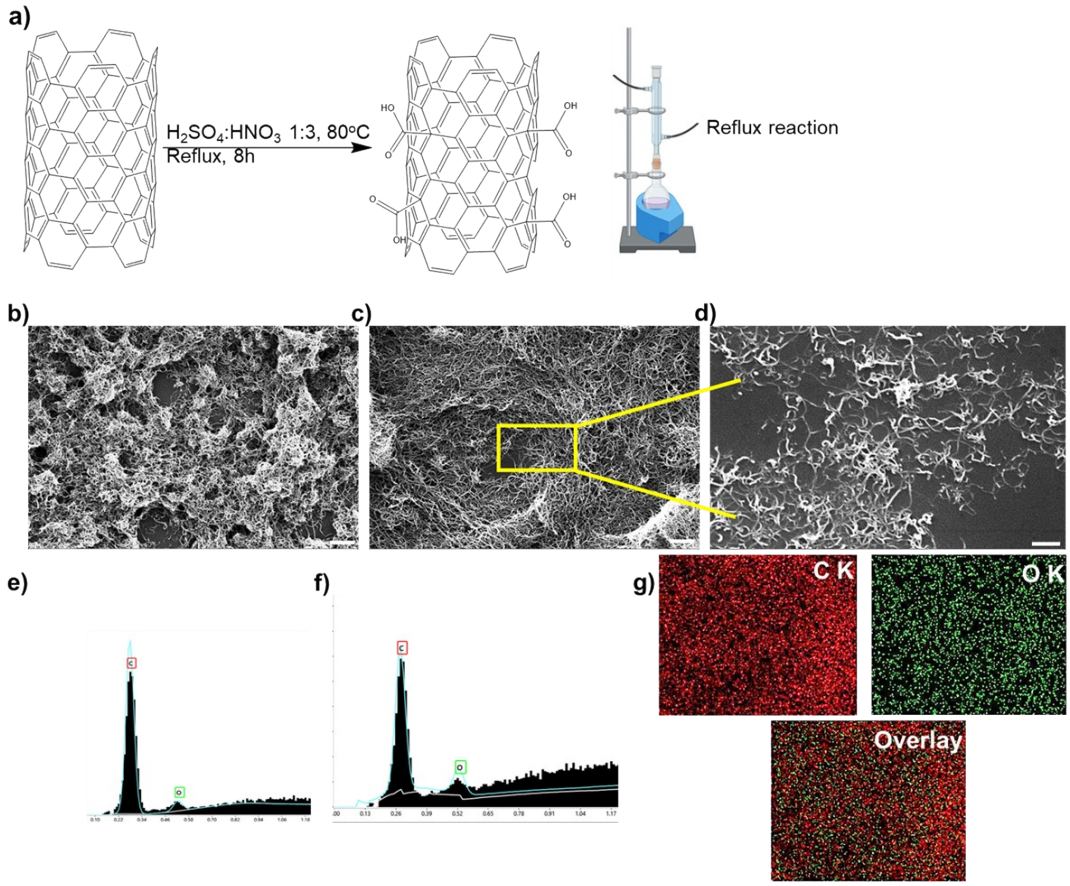

Figure S1: Acid-functionalization of CNTs and characterization. a) Schematic of the acidic oxidation of CNTs using a mixture of concentrated sulfuric and nitric acids; b, c, d) SEM micrographs of b) pristine CNTs, and f-CNTs under c) low and d) high magnifications; e, f) Elemental distribution in e) CNTs and f) f-CNTs using EDX analysis; g) Elemental mapping of C and O in the f-CNTs. (Scale: 1 µm in b, c and 500 nm in d)

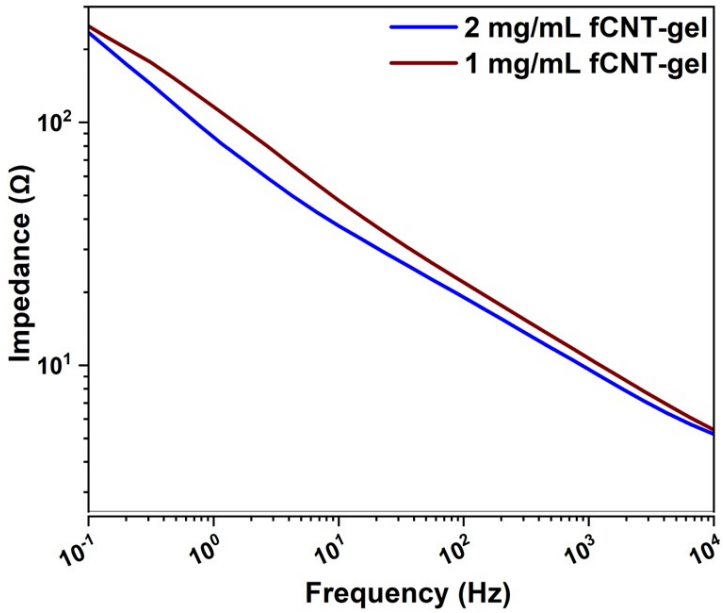

Figure S2: Impedance-frequency plots of fCNT-gel at 1 and 2 mg/mL loading of fCNT.

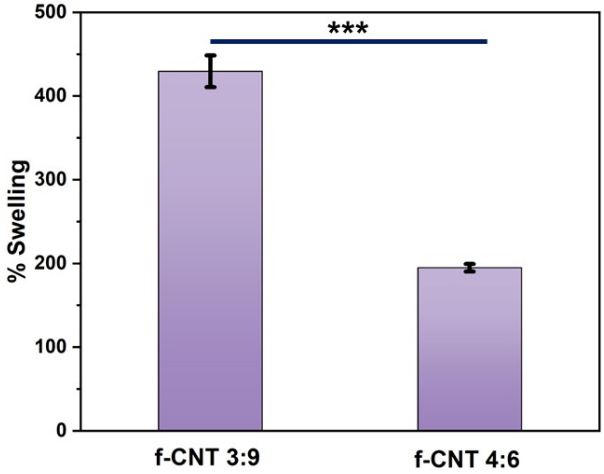

Figure S3: Estimation of the extent of swelling of fCNT-gels of two compositions in barium chloride solution post-drying.

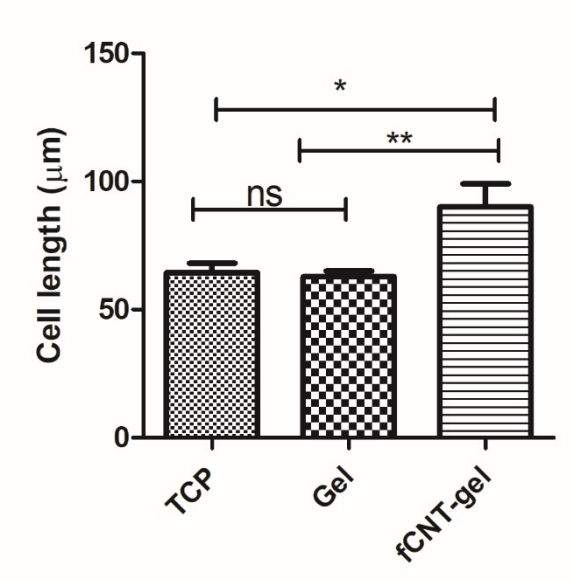

Figure S4: Cell length estimation of the HT-22 cells cultured on TCP, 3D printed gels and fCNT-gels (TCP: Tissue Culture Plate).

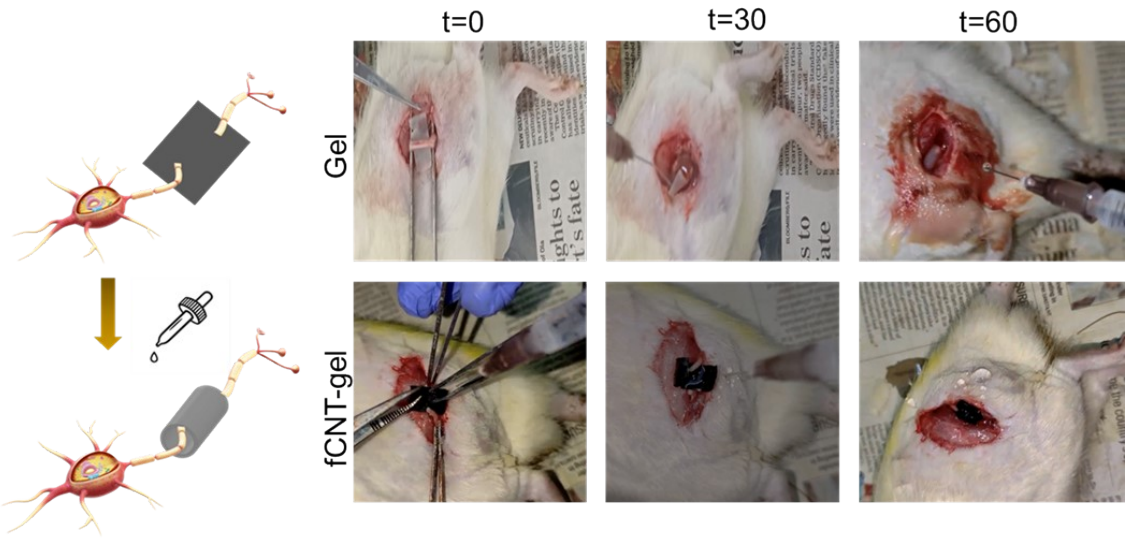

Figure S5 Schematic and experimental images of the intraoperative self-wrapping phenomenon in gel and fCNT-gel groups.

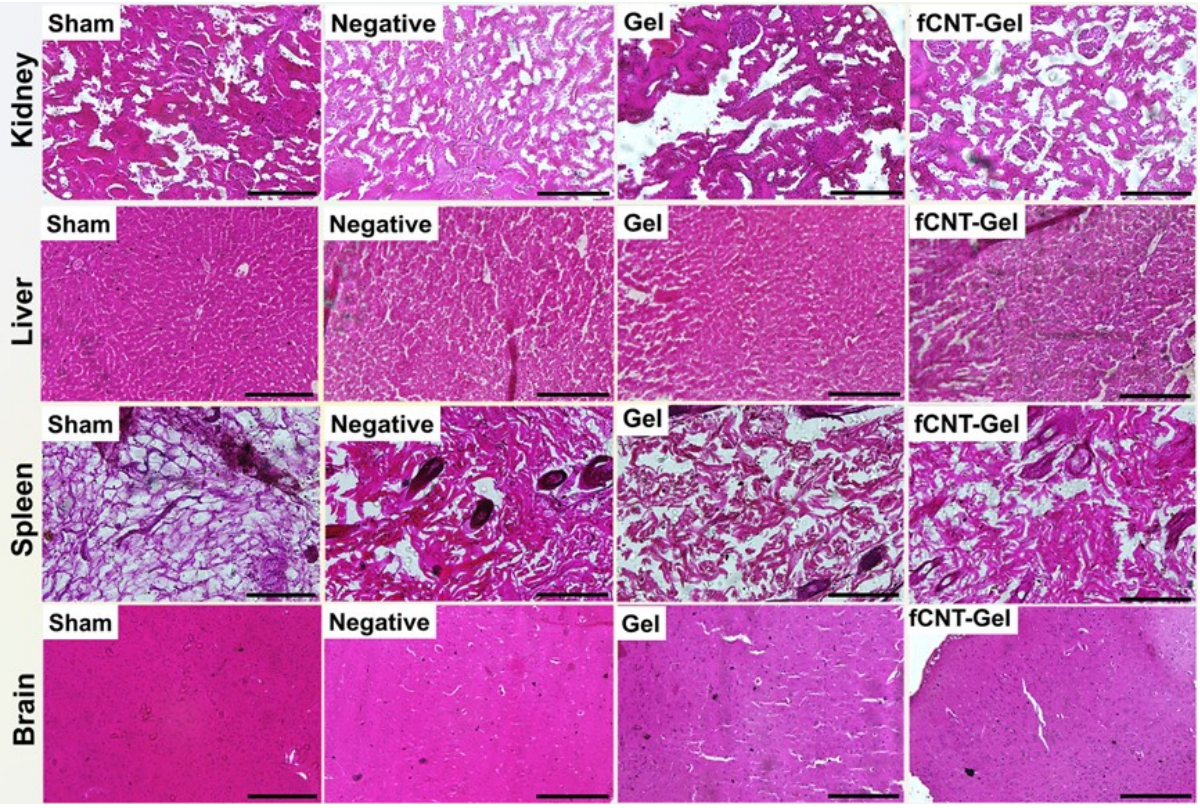

Figure S6 *In vivo* biocompatibility of the gel and fCNT-gel based NGCs 60 days post-implantation by H&E staining of the vital organs, including kidney, liver, spleen, and brain tissues in all four groups i.e. Sham, negative control, gel and fCNT-gel.

Video captions:

V1: Self-rolling of a design-encoded as-printed flat structure into a T-junction with exposure to aqueous solution

V2: Perfusion of rhodamine dye into the as-rolled T-junction without leakage

V3: Self-rolling of a flat sheet with multiple smaller tubes inside into a multi-channel hollow tube with exposure to aqueous solution